JOURNAL OF
EMERGING INVESTIGATORS

Article

Modeling stearoyl-coenzyme A desaturase 1 inhibitors to ameliorate α-Syn cytotoxicity in Parkinson's disease

Bridget Liu[*1], Audrey Tsai[*1], Darren Dressen[1]
[1] Los Altos High School, Los Altos, CA

SUMMARY

Parkinson's disease is a form of progressive neurodegeneration that primarily affects dopaminergic neurons. It is characterized by misfolded α-Synuclein (α-Syn) proteins clumped together in Lewy bodies. More recently, it has been proposed that α-Syn toxicity may increase during interactions with fatty acids. There have been several studies linking stearoyl-coenzyme A desaturase 1 (SCD1), the rate-limiting enzyme for the conversion of saturated fatty acids (SFAs) to monounsaturated fatty acids (MUFAs), to the increased toxicity of α-Syn. Consequently, SCD1 inhibition is shown to decrease the toxicity and aggregation of α-Syn. However, the precise interactions of SCD1 inhibitors and SCD1 are unclear. This project compared seven novel analogs of SCD1 inhibitors, which we hypothesized to compete with SCD1's coenzyme stearoyl coenzyme A, decreasing SFA conversion into their respective MUFAs. The analogs shared the same general pharmacophore with varying R groups (p-toluoyl, 4-fluorobenzoyl, 3-trifluoromethyl benzoyl, o-anisoyl, 3,4-difluorobenzoyl, 2-trifluoromethyl benzoyl, and 2-chlorobenzoyl). We hypothesized that analogs with the least steric hindrance would perform best. We drew a structure-activity relationship from in silico studies, with molecular docking results showing that four analogs were just as or more effective than MF-438, a commercially available SCD1 inhibitor. These results imply that the most effective R group was least sterically hindered, guiding further analog development in the field of small molecule Parkinson's disease cures.

INTRODUCTION

Parkinson's disease is a progressive neurodegenerative condition pathologically characterized by alpha-synuclein (α-Syn) aggregates in Lewy bodies and Lewy neurites (1). This aggregation leads to neuronal death, primarily of dopaminergic neurons, which synthesize the neurotransmitter dopamine (1). Clinically, this neuronal death results in impaired motor function, such as slowness of movement and muscle tremors, and non-motor symptoms, such as dementia (2). The prevalence of Parkinson's disease has been rapidly growing, doubling in the past 25 years, making it one of the fastest-growing neurological conditions worldwide (1, 3). An estimated 8.5 million people worldwide lived with Parkinson's disease in 2019, and the number is projected to grow (3). Yet, available Parkinson's disease treatments only target the disease symptoms. No treatment exists that can slow or prevent disease progression (1).

α-Syn accumulation is considered the hallmark neuropathological feature of Parkinson's disease and has been linked to neurotoxic pathways that lead to neurodegeneration (4). Because of its links to Parkinson's disease, many therapeutic efforts to create a disease-modifying treatment target α-Syn (4). In yeast, rodent, and human neuronal models, it has been shown that α-Syn triggers excess oleic acid and diglyceride production (5). More recent research has proposed α-Syn may also be a lipid-binding protein and that its physiological interactions with phospholipids and fatty acids may play a role in triggering α-Syn aggregation (6). α-Syn has a motif similar to fatty acid-binding proteins and is able to bind to oleic acid (7). These interactions may also promote α-Syn toxicity (6). Oleic acid in particular has been shown to increase α-Syn accumulation (5, 8).

Stearoyl-coenzyme A desaturase 1 (SCD1), the rate-limiting enzyme in the synthesis of monounsaturated fatty acids such as oleic acid, is a target for Parkinson's disease treatment (8). Inhibition of SCD1 decreases oleic acid production, decreasing α-Syn accumulation and α-Syn-induced toxicity as well (5, 8, 9) (Figure 1). Critically, this inhibition also increases the survival of human dopaminergic neurons (9). Successful inhibition of SCD1 in Parkinson's disease patients has the potential to slow disease progression and neuronal death.

Xenon Pharmaceuticals published the first small molecule SCD1 inhibitor in 2005, leading to a wealth of research into potential inhibitor structure, including the publication of small molecule SCD1 inhibitor MF-438 in 2010 by Merck Frosst (11, 19). However, the original lack of a crystal structure led to SCD1 inhibitor discovery through high-throughput screening and scaffold hopping instead of structure-based drug design (12). Through this method, some SCD1 inhibitors based on natural products such as 9-thiastearic acid and cyclopropenoid fatty acids were identified, but lacked potency and specificity (12, 13). Other small molecule inhibitors primarily discovered through high-throughput screening were more promising, but the lack of a crystal structure still limited the efficiency of drug discovery (12, 13). A human SCD1 crystal structure was first reported in 2015, allowing for more rational structure-based inhibitor discovery, which is more time and cost-efficient (14). With a crystal structure available, molecular docking can now be used to predict binding conformations for small molecule ligands to macromolecular targets, particularly in creating structure-activity relationships (SARs) (17).

There are few rational structure-based SCD1 inhibitor studies available, and specific SCD1 inhibitor-protein interactions are not well understood (12, 13). Here, we

https://doi.org/10.59720/23-151

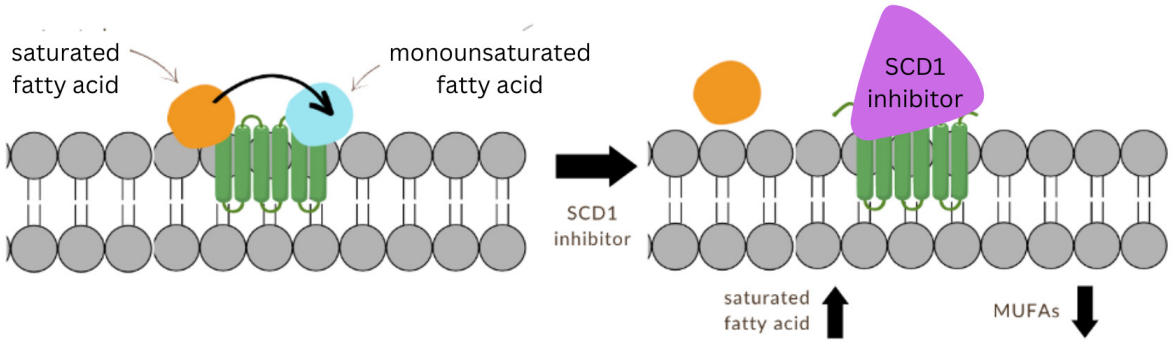

Figure 1: Function of SCD1 inhibitors. Diagram demonstrating how SCD1 converts saturated fatty acids to monounsaturated fatty acids (MUFAs). SCD1 is depicted in green, saturated fatty acids are depicted in orange, MUFAs are depicted in blue, and SCD1 inhibitor is depicted in purple.

modeled seven novel compounds as small molecule competitive SCD1 inhibitors; all analogs shared a common central pharmacophore based on previous literature and varying R groups (15) (Figure 2). The seven R groups in this study were chosen to compare the effects of fluorination, steric bulk, and benzoyl position. We hypothesized analogs with the least steric hindrance, specifically those that were fluorinated and para-substituted, would be the most effective at inhibiting SCD1. This is because substitution with fluorine can both improve analogs' metabolic stability due to the C-F bond being more resistant to attack than the C-H bond and increase binding affinity, as fluorine either interacts with the protein itself or influences surrounding groups' polarities (16). In addition, para-substituted R groups are less sterically bulky than ortho-substituted or meta-substituted R groups.

Our *in silico* molecular docking studies were conducted through Chimera and Autodock Vina to generate a SAR on how the seven varying R groups would affect analog binding affinities to SCD1. Our results showed that the best working analogs were the least sterically hindered, linear small molecules. Our best analog was the p-toluoyl analog with a binding affinity of -11.3 kcal/mol, which outperforms current commercial SCD1 inhibitors. Through our studies, SCD1 inhibitor-protein interactions were better understood, and analog efficacy was rationalized.

RESULTS

Through *in silico* modeling, we determined both the average binding affinity of each analog and drew a structure-activity relationship from the binding conformations. As reported in previous literature, ligands and proteins were downloaded from RCSB Protein Data Bank and prepped *in silico*, converted to pdbqt format, docked, and visualized with Chimera and Autodock Vina programs (18). R groups on the analogs included p-toluoyl, 4-fluorobenzoyl, 3-trifluoromethyl benzoyl, o-anisoyl, 3,4-difluorobenzoyl, 2-trifluoromethyl benzoyl, and 2-chlorobenzoyl. The control for these experiments was MF-438, a potent, orally bioavailable, and commercially available SCD1 inhibitor (19). Each analog was docked three times, and the top three binding affinities were recorded for each trial (Figure 3) (Table 1).

The more negative the affinity is, the better the ligand binds to SCD1 (20). A low binding affinity is equivalent to a binding conformation at a lower energy, where the system is thermodynamically more favorable because fewer repulsive forces are acting on the system, meaning that binding and

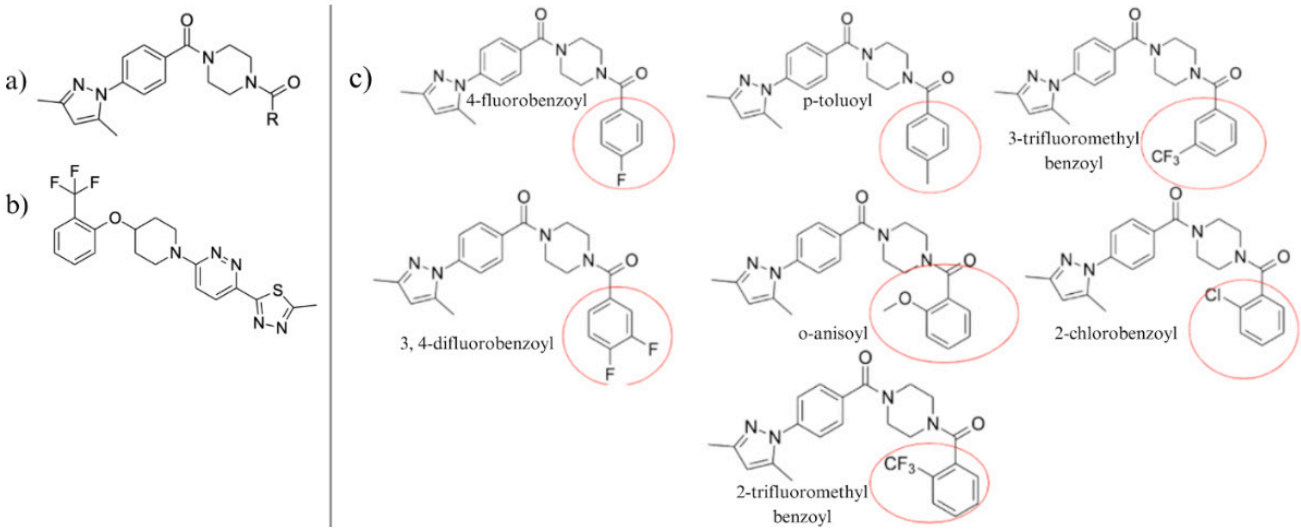

Figure 2: Chemical structures of relevant compounds. a) Analogs tested had different R groups based on this pharmacophore structure. b) MF-438, a commercially available SCD1 inhibitor and the positive control, is depicted here. c) Our seven novel SCD1 inhibitor analogs. The central pharmacophore of these analogs is shown in part b and the varying rightmost R groups are circled in red.

https://doi.org/10.59720/23-151

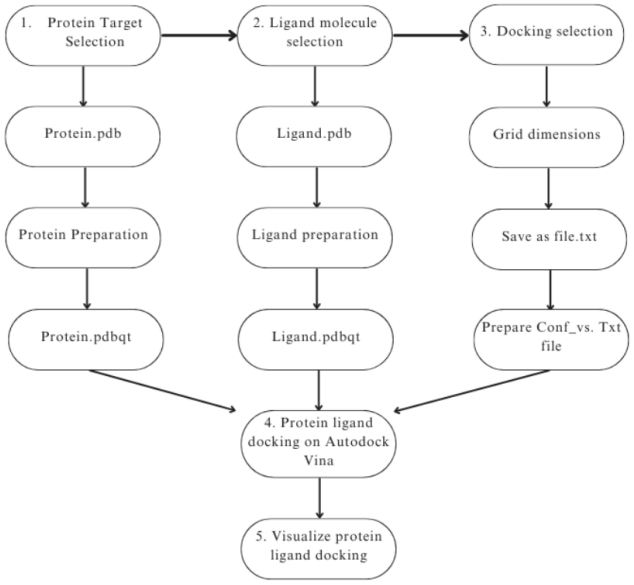

Figure 3: Molecular docking protocol summary. The generalized protocol of how each ligand was docked to our macromolecule, SCD1, is shown above. It is based on previous studies' methods elaborated in the methods section (16).

inhibition are more likely to occur (21). Thus, we aimed to find structures with low binding affinity. The analog with the best affinity of -11.6 kcal/mol was the p-toluoyl analog, the analog with the second-best affinity of -11.2 kcal/mol was the 4-fluorobenzoyl analog, and the analog that performed worst with an affinity of -8.33 kcal/mol in these molecular docking studies was the 2-chlorobenzoyl analog (Figure 4).

In addition, all seven analogs appeared to be competitive inhibitors to SCD1's substrate stearoyl-coenzyme A. All analogs bound best in place of the coenzyme substrate in the protein active site (Figure 4). It also appeared that for all seven analogs, the orientations of the best conformations had R groups facing the outside of SCD1 and the pyrazole located closer to SCD1's di-ion center. Conformations in which this orientation was reversed, with the pyrazole facing the outside of SCD1 and the R group facing SCD1's di-ion center, had worse binding affinities.

DISCUSSION

Our study investigated seven novel SCD1 inhibitors to draw a structure-activity relationship and better understand the molecular basis for SCD1 inhibition. Overall, we hypothesized that the most effective SCD1 inhibitors would have the least sterically hindered R groups and be fluorinated. The molecular docking studies conducted appeared to validate this hypothesis. The most effective analog, the p-toluoyl analog, had the best binding affinity out of all eight ligands for SCD1; this was most likely because the p-toluoyl analog had one of the least sterically hindered and smallest R groups. In addition, the second best-performing analog, the 4-fluorobenzoyl analog, had a small R group and was fluorinated, contributing to improved binding affinity. Also, fluorine-containing compounds often enhance biological activity (16). Thus, we predict this analog will perform well in future *in vitro* or *in vivo* studies.

The 2-chlorobenzoyl analog was the worst-performing analog with the highest binding affinity, likely due to steric hindrance from the bulky R-group. The large substituents attached may have interfered with binding between SCD1 and the analog (22, 23). Moreover, the difference between the same substituents at different positions on the benzoyl ring (3-trifluoromethyl and 2-trifluoromethyl) producing different binding affinities supported the hypothesis that small analogs with little steric bulk perform better than sterically bulky ones. Future studies may want to focus on R groups attached to the third carbon, as the R group is positioned further away from the rest of the analog to decrease steric hindrance, allowing for a better fit in the binding pocket. The pyrazole-end of our analogs appeared to be responsible for making contact with the active site.

Our *in silico* studies also appeared to show that four out of seven of our analogs (4-fluorobenzoyl, p-toluoyl, 3-trifluoromethyl, and o-anisoyl) were just as or more effective than MF-438. This is again hypothesized to be due to the large steric bulk of MF-438 compared to these analogs, as MF-438 has a trifluoromethyl group equivalent to its R group. In addition, MF-438 performed equally as well as our 3-trifluoromethyl benzoyl analog; both share the same R group.

In terms of a trend forming where conformations with the pyrazole facing the di-ion center and R group facing oppositely perform better than analogs with the opposite

Analog	Trial 1 Binding Affinity (kcal/ml)	Trial 2 Binding Affinity (kcal/ml)	Trial 3 Binding Affinity (kcal/ml)	Average Binding Affinity (kcal/ml)
MF438 (control)	-10.6	-10.6	-10.6	**-10.6**
	-10	-9.9	-9.9	-9.9
	-9.8	-9.8	-9.8	-9.8
p-toluoyl	-11.3	-11.3	-11.3	**-11.3**
	-10.6	-9	-9	-9.53
	-9.8	-8.7	-8.7	-9.07
4-fluorobenzoyl	-11.2	-11.1	-11.2	**-11.2**
	-9	-8.8	-10.6	-9.47
	-8.9	-8.6	-8.9	-8.8
3-trifluoromethyl benzoyl	-10.6	-10.5	-10.6	**-10.6**
	-9.4	-10	-9.4	-9.6
	-8.4	-9.8	-8.8	-9
o-anisoyl	-10.6	-10.6	-10.6	**-10.6**
	-8.3	-8.1	-9.5	-8.63
3, 4-difluorobenzoyl	-10.2	-10.2	-10.2	**-10.2**
	-10	-10.1	-10.1	-10.1
	-9.8	-9.8	-10	-9.9
2-trifluoromethyl benzoyl	-9.9	-10	-10	**-9.97**
	-8.9	-9.1	-8.9	-8.97
	-8.8	-9.1	-8.7	-8.87
2-chlorobenzoyl	-7.1	-10.8	-7.1	**-8.33**
	-6.9	-9.3	-6.9	-7.7
	-6.7		-6.8	-6.75

Table 1: Top three binding affinities of ligands towards SCD1. Calculated binding affinities in kcal/mol of each ligand for the macromolecule SCD1 are shown using the software Autodock Vina and the method described in molecular docking studies. Aside from the control (MF-438) in row one, analogs are listed from lowest to highest binding affinities. The top three binding conformations are listed for each analog, in order of lowest to highest binding affinities. Only two possible conformations were generated per trial for o-anisoyl and trial two of 2-chlorobenzoyl.

https://doi.org/10.59720/23-151

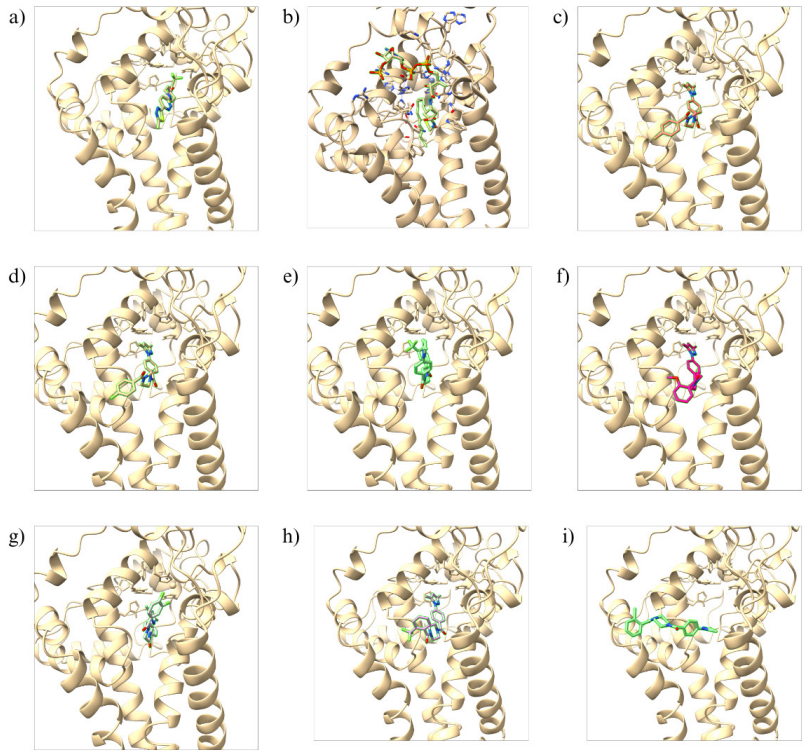

Figure 4: SCD1 inhibitors docked to SCD1. MF-438 (a), stearoyl coenzyme A (b), the naturally occurring substrate for SCD1, and all seven analogs (c-i), organized from most to least negative of top binding affinities over all three trials, are highlighted in green and docked to SCD1. The top binding conformations are shown for (a) MF-438, (b) stearoyl coenzyme A, (c) p-toluoyl, (d) 4-fluorobenzoyl, (e) 3-trifluoromethyl benzoyl, (f) o-anisoyl, (g) 3,4-difluorobenzoyl, (h) 2-trifluoromethyl benzoyl, (i) 2-chlorobenzoyl.

conformation, we hypothesize that this is because the R group does not actually participate in binding. Thus, its exact structure may not be as important; what matters is that the R group provides low steric hindrance to make the overall system's potential energy as negative as possible, making it more thermodynamically favorable. To further investigate this matter, molecular docking should also be conducted on analogs where R groups are consistent and the pyrazole changes.

In addition, it was interesting to note that although the 3-trifluoromethyl and 2-trifluoromethyl analogs shared the same R group, the difference in the R group's position on the benzoyl led to a notable difference in binding affinity, as the 3-trifluoromethyl analog performed better than its counterpart (Table 1).

Other possible limitations include those of the Chimera and Autodock Vina programs used in this paper. The maximum energy difference between conformations is 3 kcal/mol, meaning binding modes with scores over 3 kcal/mol greater than the lowest binding affinity generated for an analog are not included in Autodock Vina results (24). That is why o-anisoyl only has two binding conformations for all three trials, and trial two for 2-chlorobenzoyl only has two binding conformations. In addition, AutoDock is limited in that it lacks receptor flexibility, using a rigid SCD1 receptor model instead of a flexible binding model. Tools that account for conformational receptor changes and molecular dynamic methods are more realistic and may yield more accurate results (25).

More importantly, because all of our analogs bound to SCD1 in *in silico* studies, these novel analogs hold the potential to be potent SCD1 inhibitors. And, as SCD1 inhibitors, they also hold the potential to mitigate the symptoms of Parkinson's disease and slow the disease's progression. However, *in vitro* and *in vivo* assays should also be conducted to support our hypothesis. Future research should focus on bioassays guided by the results in this paper. Testing our analogs in cells and comparing the levels of their saturated fatty acids and MUFAs via liquid chromatography-mass spectrometry (LC-MS) is one example that would provide *in vitro* evidence to support our docking studies. For example, previous studies have used mice models with Parkinson's disease and LC-MS to observe lipid levels (26). Our work contributes to future SCD1 development in the realm of small-molecule Parkinson's disease treatments, guiding future structure-based SCD1 inhibitor design.

MATERIALS AND METHODS

First, the SCD1 protein crystal structure was retrieved from the Protein Data Bank and downloaded as a pdb file (Figure 3) (27). In Chimera, all unnecessary protein chains, additional ligands, water, and heteroatoms were deleted; polar hydrogens were added; missing atoms were checked for; and Kollman charges were added and spread equally. This prepped macromolecule was then saved as a pdbqt file.

Second, to prepare ligands for docking, the control MF-438 and experimental analogs were separately processed. MF-438 was retrieved from the PubChem database and downloaded in sdf format (28). In PyMol, this file was then converted to a pdb format. It was then prepared in Autodock

https://doi.org/10.59720/23-151

Tools by adding Gasteiger charges and saved as a pdbqt file. For experimental analogs, molecules were created in Avogadro and geometrically optimized, and then prepared in Autodock Tools using the same method as the control ligand.

Third, a gridbox for the pocket site of protein docking was chosen, with dimensions having a spacing of 20 in the x-direction, 20 in the y-direction, and 30 in the z-direction, and a center with x-coordinate 15, y-coordinate 70, and z-coordinate 45.

Lastly, the protein-ligand docking was performed with Chimera using the built-in Autodock Vina feature. Output .pdbqt and log files were then generated and visualized in ChimeraX. All analogs and MF-438 were docked to SCD1 three times, with binding affinities recorded for the top three binding conformations, which were then separately averaged.

ACKNOWLEDGEMENTS

We thank Dr. Njoo and Dr. Santoros for guiding our chemistry efforts and Dr. Johnson for assisting our biological efforts. Lastly, we thank Los Altos High School and the Advanced Science Investigations class for allowing us to conduct our research there.

Received: July 8, 2023
Accepted: August 23, 2023
Published: June 25, 2024

REFERENCES

1. Bloem, Bastiaan R., et al. "Parkinson's Disease." *The Lancet*, vol. 397, no. 10291, June 2021, pp. 2284–303. *ScienceDirect*, https://doi.org/10.1016/S0140-6736(21)00218-X.
2. Sveinbjornsdottir, Sigurlaug. "The Clinical Symptoms of Parkinson's Disease." *Journal of Neurochemistry*, vol. 139, no. S1, 2016, pp. 318–24. *Wiley Online Library*, https://doi.org/10.1111/jnc.13691.
3. "Launch of WHO's Parkinson Disease Technical Brief." *Who.int*, World Health Organization: WHO, 14 June 2022.
4. Fields, Carroll Rutherford, et al. "Targeting Alpha-Synuclein as a Therapy for Parkinson's Disease." *Frontiers in Molecular Neuroscience*, vol. 12, 2019. *Frontiers*, https://doi.org/10.3389/fnmol.2019.00299.
5. Fanning, Saranna, et al. "Lipidomic Analysis of α-Synuclein Neurotoxicity Identifies Stearoyl CoA Desaturase as a Target for Parkinson Treatment." *Molecular Cell*, vol. 73, no. 5, Mar. 2019, pp. 1001-1014.e8. *ScienceDirect*, https://doi.org/10.1016/j.molcel.2018.11.028.
6. Fanning, Saranna, et al. "Parkinson's Disease: Proteinopathy or Lipidopathy?" *Npj Parkinson's Disease*, vol. 6, no. 1, 1, Jan. 2020, pp. 1–9. *www.nature.com*, https://doi.org/10.1038/s41531-019-0103-7.
7. Xicoy, Helena, et al. "The Role of Lipids in Parkinson's Disease." *Cells*, vol. 8, no. 1, 1, Jan. 2019, p. 27. *www.mdpi.com*, https://doi.org/10.3390/cells8010027.
8. Nicholatos, Justin W., et al. "SCD Inhibition Protects from α-Synuclein-Induced Neurotoxicity But Is Toxic to Early Neuron Cultures." *ENeuro*, vol. 8, no. 4, July 2021. *www.eneuro.org*, https://doi.org/10.1523/ENEURO.0166-21.2021.
9. Vincent, Benjamin M., et al. "Inhibiting Stearoyl-CoA Desaturase Ameliorates α-Synuclein Cytotoxicity." *Cell Reports*, vol. 25, no. 10, Dec. 2018, pp. 2742-2754.e31. *ScienceDirect*, https://doi.org/10.1016/j.celrep.2018.11.028.
10. Brown, J. M.; Rudel, L. L. Stearoyl-Coenzyme A Desaturase 1 Inhibition and the Metabolic Syndrome: Considerations for Future Drug Discovery. *Curr Opin Lipidol* **2010**, *21* (3), 192–197. https://doi.org/10.1097/MOL.0b013e32833854ac.
11. Chakka, N.; et al. Pyridazine Derivatives and Their Use as Therapeutic Agents. WO2006086447A3, April 5, 2007.
12. Liu, G. Stearoyl-CoA Desaturase Inhibitors: Update on Patented Compounds. *Expert Opinion on Therapeutic Patents* **2009**, *19* (9), 1169–1191. https://doi.org/10.1517/13543770903061311.
13. Uto, Y. Recent Progress in the Discovery and Development of Stearoyl CoA Desaturase Inhibitors. *Chemistry and Physics of Lipids* **2016**, *197*, 3–12. https://doi.org/10.1016/j.chemphyslip.2015.08.018.
14. Wang, H.; Klein, M. G.; Zou, H.; Lane, W.; Snell, G.; Levin, I.; Li, K.; Sang, B.-C. Crystal Structure of Human Stearoyl–Coenzyme A Desaturase in Complex with Substrate. *Nat Struct Mol Biol* **2015**, *22* (7), 581–585. https://doi.org/10.1038/nsmb.3049.
15. Zhang, Zaihui, et al. "Opportunities and Challenges in Developing Stearoyl-Coenzyme A Desaturase-1 Inhibitors as Novel Therapeutics for Human Disease." *Journal of Medicinal Chemistry*, vol. 57, no. 12, June 2014, pp. 5039–56. *ACS Publications*, https://doi.org/10.1021/jm401516c.
16. Shah, Poonam, and Andrew D. Westwell. "The Role of Fluorine in Medicinal Chemistry." *Journal of Enzyme Inhibition and Medicinal Chemistry*, vol. 22, no. 5, Jan. 2007, pp. 527–40. *Taylor and Francis+NEJM*, https://doi.org/10.1080/14756360701425014.
17. Forli, Stefano, et al. "Computational Protein–Ligand Docking and Virtual Drug Screening with the AutoDock Suite." *Nature Protocols*, vol. 11, no. 5, 5, May 2016, pp. 905–19. *www.nature.com*, https://doi.org/10.1038/nprot.2016.051.
18. Aqeel, Imra, et al. *Drug Repurposing For SARS-COV-2 Using Molecular Docking*. arXiv:2206.01047, arXiv, 26 July 2022. *arXiv.org*, https://doi.org/10.48550/arXiv.2206.01047.
19. Léger, Serge, et al. "Synthesis and Biological Activity of a Potent and Orally Bioavailable SCD Inhibitor (MF-438)." *Bioorganic & Medicinal Chemistry Letters*, vol. 20, no. 2, Jan. 2010, pp. 499–502. *ScienceDirect*, https://doi.org/10.1016/j.bmcl.2009.11.111.
20. Xue, Qiao, et al. "Evaluation of the Binding Performance of Flavonoids to Estrogen Receptor Alpha by Autodock, Autodock Vina and Surflex-Dock." *Ecotoxicology and Environmental Safety*, vol. 233, Mar. 2022, p. 113323. *ScienceDirect*, https://doi.org/10.1016/j.ecoenv.2022.113323.
21. Fadlan, A.; Nusantoro, Y. R. The Effect of Energy Minimization on The Molecular Docking of Acetone-Based Oxindole Derivatives. *JKPK (Jurnal Kimia dan Pendidikan Kimia)* 2021, *6* (1), 69–77. https://doi.org/10.20961/jkpk.v6i1.45467.
22. Hlavacek, William S., et al. "Steric Effects on Multivalent Ligand-Receptor Binding: Exclusion of Ligand Sites by

https://doi.org/10.59720/23-151

Bound Cell Surface Receptors." *Biophysical Journal*, vol. 76, no. 6, June 1999, pp. 3031–43. *ScienceDirect*, https://doi.org/10.1016/S0006-3495(99)77456-4.
23. Liu, Shubin, et al. "Steric, Quantum, and Electrostatic Effects on SN2 Reaction Barriers in Gas Phase." *The Journal of Physical Chemistry A*, vol. 114, no. 18, May 2010, pp. 5913–18. *ACS Publications*, https://doi.org/10.1021/jp101329f.
24. Trott, O.; Olson, A. J. AutoDock Vina: Improving the Speed and Accuracy of Docking with a New Scoring Function, Efficient Optimization and Multithreading. *J Comput Chem* **2010**, *31* (2), 455–461. https://doi.org/10.1002/jcc.21334.
25. Forli, S.; Huey, R.; Pique, M. E.; Sanner, M.; Goodsell, D. S.; Olson, A. J. Computational Protein-Ligand Docking and Virtual Drug Screening with the AutoDock Suite. *Nat Protoc* **2016**, *11* (5), 905–919. https://doi.org/10.1038/nprot.2016.051.
26. Nuber, S.; Nam, A. Y.; Rajsombath, M. M.; Cirka, H.; Hronowski, X.; Wang, J.; Hodgetts, K.; Kalinichenko, L. S.; Müller, C. P.; Lambrecht, V.; Winkler, J.; Weihofen, A.; Imberdis, T.; Dettmer, U.; Fanning, S.; Selkoe, D. J. A Stearoyl–Coenzyme A Desaturase Inhibitor Prevents Multiple Parkinson Disease Phenotypes in A-Synuclein Mice. *Ann Neurol* **2021**, *89* (1), 74–90. https://doi.org/10.1002/ana.25920.
27. *RCSB PDB - 4ZYO: Crystal Structure of Human Integral Membrane Stearoyl-CoA Desaturase with Substrate*.
28. PubChem. *2-Methyl-5-(6-(4-(2-(Trifluoromethyl) Phenoxy)Piperidin-1-Yl)Pyridazin-3-Yl)-1,3,4-Thiadiazole*.